



DEVELOPMENT OF A THERMAL MATHEMATICAL MODEL FOR THE SIMULATION OF TRANSIENT BEHAVIOR OF A SPACEBORNE EQUIPMENT IN VACUUM ENVIRONMENT

Cem ÖMÜR* and Ahmet Bilge UYGUR**

* Turkish Aerospace Industries, Inc., Fethiye Mah. Havacılık Blv. No:17. 06980, Ankara, comur@tai.com.tr

** Turkish Aerospace Industries, Inc., Fethiye Mah. Havacılık Blv. No:17. 06980, Ankara, auygur@tai.com.tr

(Geliş Tarihi: 13.08.2014, Kabul Tarihi: 16.12.2014)

Abstract: This paper focuses on the development of a thermal mathematical model representing a spaceborne electronic equipment in thermal vacuum test environment. The model was based on Thermal Network Method (TNM). Simulations with the model were carried out using a commercial thermal analysis software package. The predictions obtained with the model were compared with the thermal vacuum cycling test measurements. Transient standard deviations between the predictions and the test measurements show that the mathematical model developed was able to represent the thermal vacuum environment accurately and it can be utilized in the design phases of similar spaceborne equipment.

Keywords: Thermal vacuum cycling test, Thermal vacuum chamber (TVC), Spaceborne equipment, Thermal network method (TNM), Printed circuit board (PCB)

UZAY ORTAMINDA KULLANILAN BİR ELEKTRONİK EKİPMANIN VAKUM ORTAMINDA ZAMANA BAĞLI DAVRANIŞININ BENZETİMİ İÇİN ISIL MATEMATİKSEL MODEL GELİŞTİRİLMESİ

Özet: Bu makalede, ısıl vakum test ortamındaki uzay ortamında kullanılan bir elektronik ekipmanını temsil eden ısıl matematiksel modelin geliştirilmesi üzerinde durulmuştur. Model, Isıl Ağ Metod'una dayalıdır. Bu modelin kullanıldığı benzetimler ticari bir ısıl analiz yazılım paketi kullanılarak gerçekleştirilmiştir. Modelden elde edilen zamana bağlı öngörüler ısıl vakum döngü testi sonuçlarıyla karşılaştırılmıştır. Öngörüler ve ölçümler arasında hesaplanan zamana bağlı standart sapmalar, geliştirilen matematiksel modelin ısıl vakumu ortamını doğru bir şekilde temsil edebildiğini ve bu modelin benzer uzay ortamında kullanılacak elektronik ekipmanların tasarım aşamalarında kullanılabileceğini göstermiştir.

Anahtar Kelimeler: Isıl vakum döngü testi, Isıl vakum odası, Uzay ortamında kullanılan elektronik ekipman, Isıl ağ metodu, Baskı devre kartı

NOMENCLATURE

ρ	Density (kg/m ³)
σ	Stefan-Boltzman constant (W/m ² ·K ⁴)
τ	Radiative exchange factor
A	Area (m ²)
C	Conductive conductor (W/K)
c_p	Specific heat at constant pressure (J/kg·K)
G	Total Conductor (W/K)
k	Thermal conductivity (W/m.K)
L	Distance (m)
m	Mass (kg)
N	Total number of nodes
q	Heat transfer rate (W)
q_C''	Conductive heat flux (W/m ²)
q_R''	Radiative heat flux (W/m ²)
q'''	Source term per unit volume (W/m ³)
R	Radiative conductor (W/K ⁴)
t	Time (s)
T	Temperature (K)

Subscripts

i	Node i
j	Node j

Superscripts

c	Conduction
r	Radiation

INTRODUCTION

One of the most critical issues in the design of electronic equipment is the characterization of its thermal behavior. For this purpose, utilization of thermal mathematical models and experimental techniques are commonly practiced strategies. In a study by Kim et al. (Kim et al., 2009), an electro-thermal model describing the dynamic thermal behavior of an electronic device in a test enclosure filled with air was developed. The model was able to predict the thermal contact resistances based on the temperature difference between the components of the printed circuit board (PCB) and the air temperature

measured inside the enclosure. Sartre et al. (Sartre et al., 2001) on the other hand investigated the enhancement of thermal conductance between electronic components and heat sinks. Various interstitial materials (greases and thermal fillers) suitable for the thermal enhancement in electronic systems were tested with the varying torques providing compression on the electrical component and filler. Results showed that the most influential parameter is the applied torque.

Despite providing useful information in terms of thermal characterization, both of the aforementioned studies were performed under ambient conditions and their applicability to spaceborne equipment are limited. Space environment however, imposes severe conditions on the equipment such as vacuum. Therefore, performing tests under conditions similar to the working environment of the spaceborne equipment is necessary. In accordance with this, Quinterro et al. (Quinterro et al., 1999) examined different heat transfer mechanisms that operate in thermal vacuum cycling and ambient thermal cycling tests. It was found that testing under vacuum is indispensable for detection of failures and characterization of the thermal behavior of the spaceborne equipment. Similarly, Seo et al. (Seo et al., 2013) investigated the thermal failure of the LM117 regulator used in the transponder unit of the Korean LEO Earth Observation satellite in vacuum environment. A simple thermal mathematical model based on thermal networks was developed at the component level without including radiative heat transfer. The analysis performed using test data and the model showed that in order to prevent the LM117 regulator to reach 150 °C (and shut down the system) a sufficient "finger pressure" must be applied to the thermal filler between the LM117 regulator and the PCB.

The present study focuses on the development of an extensive thermal mathematical model which governs the transient thermal behavior of an Attitude Determination Control Unit (ADCU) in thermal vacuum chamber (TVC) environment. The model is based on thermal network method (TNM) (Oppenheim, 1954) and includes both radiative and conductive heat transfer mechanisms. The simulations with the model were carried out by using THERMICA-MS SINDA software package. The validation of the model was performed by comparing its predictions with the thermal vacuum cycling test (TVCT) data.

DESCRIPTION OF THE PHYSICAL SYSTEM

The physical system to be modeled consists of the thermal vacuum chamber which is the test system and the ADCU which is the device under test.

Thermal Vacuum Chamber

The TVC test facility shown in Fig. 1 consists of the following elements:

- Vessel: The enclosed volume in which tested device is kept under vacuum.

- Shroud: The The temperature controlled radiative heat sink/source. It utilizes conventional fluid circulation to achieve temperatures ranging from -60 °C to 120 °C.
- Mounting plate: The The element on which the device under test is mounted.
- Temperature sensors: Pt100 type temperature sensor.

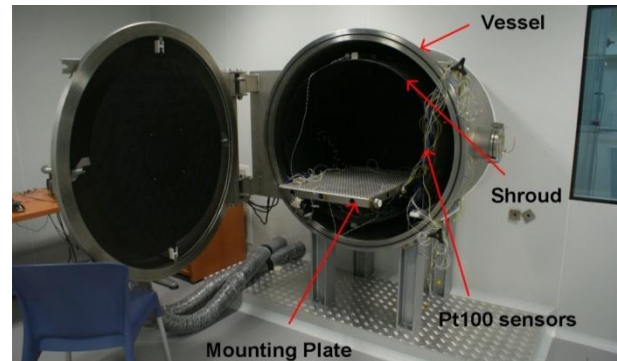


Figure 1. Thermal vacuum chamber

The TVC test facility shown in Fig. 1 consists of the following elements:

- Shroud diameter: 800 mm
- Shroud length: 720 mm
- Emissivity of the shroud: 0.88±0.04
- Shroud temperature ramp rate: 1 °C/min
- Mounting plate : 480 mm × 660 mm × 2 mm
- Pressure: <10⁻⁵ mbar
- Max. temperature difference along the shroud: 0.5 °C

The ADCU

The ADCU shown in Fig.2, is an electronic device composed of a PCB and an enclosing aluminum rectangular box. It works as an interface board between the sensors (the solar sensor, the magnetometer, the magnetic torque bars) and the controller-area network. ADCU translates the measurement data of the sensors into the digital format and transmits it to controller-area network.

The box and the PCB have dimensions of 294 x 322 x 38 mm and 288 x 316 x 2 mm, respectively. The PCB is fixed to the box using thirty (30) M2.5x5 screws whereas five (5) M6x6 bolts are used for fixing the box to the mounting plate of the TVC.

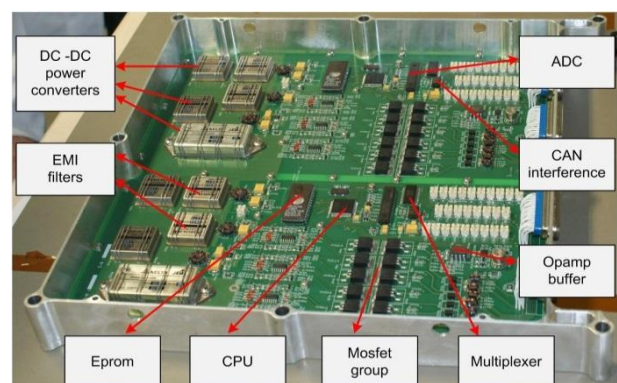


Figure 2. Layout of the ADCU

DESCRIPTION OF THE PHYSICAL SYSTEM

Governing Equation

The physical system under consideration consists of an electronic box on a mounting plate both of which are located inside a cylindrical volume that is kept under vacuum. Hence the mathematical modeling of this system necessitates the solution of energy equation in the absence of convective heat transfer which can be written as

$$\rho C_p \frac{\partial T}{\partial t} = -\nabla \cdot q_c'' - \nabla \cdot q_r'' + q''' \quad (1)$$

where ρ is the density, C_p is the specific heat, T is the temperature and t is the time. The term on the left side is the rate of change of energy stored within a unit volume. The first term on the right-hand-side $-\nabla \cdot q_c''$ is the rate of energy loss per unit volume by heat conduction whereas the second term $-\nabla \cdot q_r''$ is the rate of energy loss per unit volume by radiative heat transfer. The last term q''' accounts for the source term per unit volume.

Thermal Network Method

The Thermal Network Method is the representation of a system by cell-centered nodes and resistances amongst these nodes using finite difference method. Application of TNM to Eq. (1) yields the following discrete form of the energy equation

$$\frac{\partial T_i}{\partial t} \approx \frac{1}{(mc_p)_i} \left[\sum_{j=1}^N C_{i,j} (T_j - T_i) + \sum_{j=1}^N R_{i,j} (T_j^4 - T_i^4) \right] + \frac{q_i}{(mc_p)_i} \quad i = 1, \dots, N \quad (2)$$

In Eq. (2), $R_{i,j}$ is the radiation conductor (reciprocal of radiative resistance between nodes i and j) which can be expressed by

$$R_{i,j} = \sigma A_i^r \tau_{i,j} \quad (3)$$

where σ is the Stephan-Boltzman constant, A_i^r is the radiative heat transfer area and $\tau_{i,j}$ is the radiative exchange factor (Siegel and Howell, 2002) which accounts for the net amount of radiative energy emitted by node i and received by node j and is a function of the geometric view factors between the nodes. In this study, calculation of geometric view factors and the resulting radiation exchange factors were carried out by THERMICA software (Astrium, 2003). $C_{i,j}$ in Eq. (2) is the linear conductive conductor (reciprocal of the conductive resistance between nodes i, j) and defined as

$$C_{i,j} = \frac{k_{i,j} A_i^c}{L_{i,j}} \quad (4)$$

where, $k_{i,j}$ is the effective thermal conductivity between node i and j , A_i^c is the conduction area of between node

i and j , $L_{i,j}$ is the distance between node i and j . Eq. (4) can be used for the computation of homogenous conductors i.e. for nodes that are on the same surface. However, most of the conductors in the system under consideration cannot be treated as homogenous and hence their computation necessitates the use of thermal contact resistances. In such cases, the conduction conductor is calculated by taking the reciprocal of the contact resistance between the two surfaces, details of which will be explained in the next section.

Computation of conduction conductors by using thermal contact resistances

Within the scope of this paper, special attention is devoted to the computation of conductive conductors, thermal contact resistances in particular which constitutes the core of this modeling effort. There are four different types of contact resistances encountered in the physical system which are illustrated in Fig. 3.

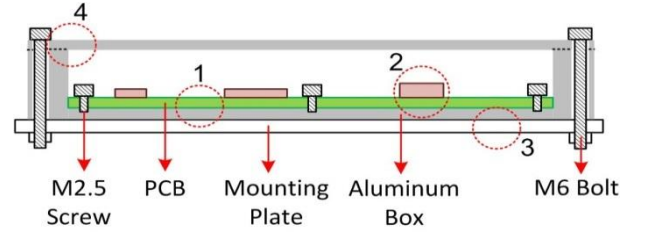


Figure 3. Types of contact resistances

The first type of contact is the one occurring between PCB and the aluminum box (see Fig. 3). PCB is fixed to the box using thirty (30) M2.5 screws. In order to calculate this contact resistance, a diagram provided by Gilmore (2002) which provides overall heat transfer coefficient as a function of inverse of screw density (cm^2/screw) is utilized. An overall heat transfer coefficient of 95 W/K.m^2 is obtained from this source with the assumptions that the system is under vacuum, plates are relatively thin ($\approx 2 \text{ mm}$), the aluminum box has a bare clean surface finish and the screws are torqued to their standard values. The overall heat transfer coefficient found was then converted to conductors by multiplying it with the contact areas.

The second type of contact is encountered between PCB and the electronic components. The components are bound to the PCB by means of Sargon 25G-Tag thermal fillers manufactured by Fujipoly (2009) having a contact resistance of $2.25 \text{ K-cm}^2/\text{W}$. For the computation of this type of conductor, the inverse of contact resistance is multiplied by the electronic component base area.

The third type of contact is due to the interface between the aluminum box and the stainless steel mounting plate. Five (5) M6x6 bolts were used for fixing the box to the mounting plate. For this, Gilmore (2002) suggests the use of a diagram which shows heat transfer coefficient vs. contact pressure. A heat transfer coefficient of 80 W/K.m^2 was selected based on the facts that the contact occurs in vacuum, the materials have wavy surface finish

with a contact pressure of 1200 kPa. The conductors are calculated by multiplying the selected heat transfer coefficient with the contact area.

Fourth and the last type of the contact resistance arises due to the interface between the box and its cover plate. For this type of contact, a heat transfer coefficient of 850 W/K.m² was selected by using the same diagram that has been utilized for the the third contact type but with different criteria: contact occurs in vacuum between same type of metals (aluminum 7075 to aluminum 7075) having smooth surface finish (0.2-0.5 μm) which accounts for the difference between the heat transfer coefficients of the third and fourth type of contacts.

Geometrical Model and its Decomposition to Thermal Nodes

The geometrical representation of the problem under consideration and its decomposition to thermal nodes are illustrated in Fig.4. The geometrical model consists of the following elements:

- Shrouds: The cylindrical volume enclosed by shrouds is represented by a cylindrical surface and two discs (3 elements). Shrouds act as heat sink and the maximum temperature variation on them is 0.5 °C. Therefore each shroud element is treated as boundary node and represented by a single thermal node.
- Mounting plate: The mounting plate is thermally and geometrically decoupled from the shrouds and represented by a single rectangular surface having 4×4 thermal nodes. The holes on the mounting plate are not represented in the geometrical model but their effect is taken into account in the calculation of heat capacities of the thermal nodes of the mounting plate.
- Aluminum Box: It is represented by six rectangular surfaces. Top and bottom surfaces are divided into 16 thermal nodes whereas side surfaces are divided into 4 thermal nodes.
- PCB: The PCB and its components are represented by rectangular surfaces. The PCB itself is divided into 4×4 thermal nodes whereas the components are represented by a single thermal node. The heat dissipations from the components of the PCB while the ADCU is in operation are tabulated in Table 1. Components such as multiplexer, Mosfet, and EMI filters are not taken into account due to their negligible heat dissipations (~0.001 W).

Table 1: Maximum heat dissipation of thermal nodes on the PCB

Node number	Component name	Heat dissipations (W)
84	Power converter	1.268
85	Power converter	1.268
86	Power converter	2.536
87	Power converter	1.268

88	Power converter	1.268
89	Power converter	2.536
90	Eprom	0.125
91	CPU	0.100
92	ADC	0.120
93	Canbus interference	0.090
94	Opamp buffer	0.360
95	Eprom	0.125
96	CPU	0.100
97	ADC	0.120
98	Canbus interference	0.090
99	Opamp buffer	0.360

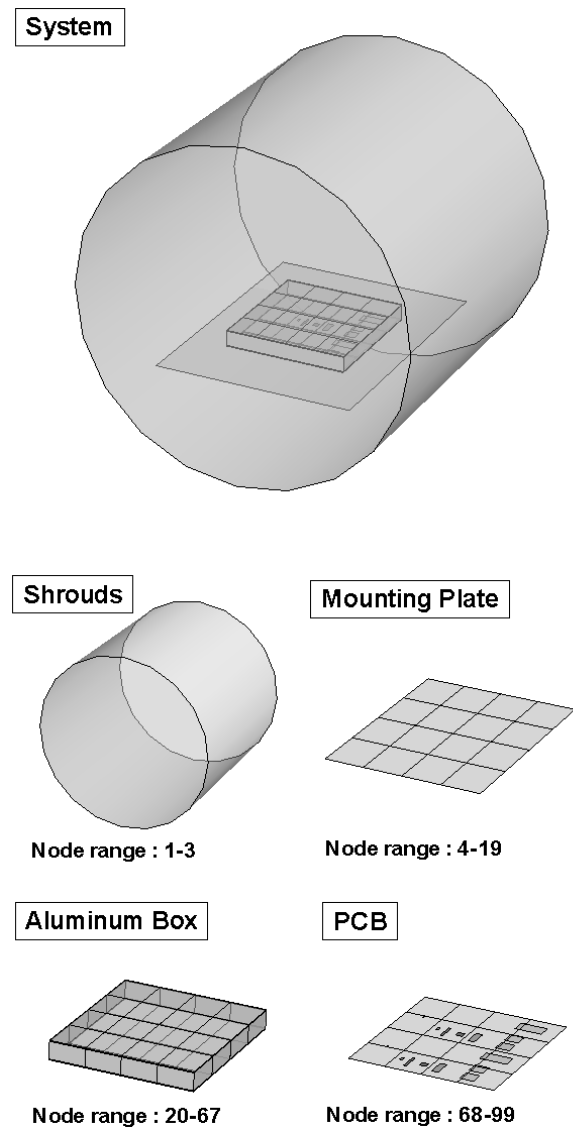


Figure 4. Geometrical model

Numerical Solution Technique

For the transient solution of the problem under consideration, THERMICA & MSC SINDA software package developed by Astrium (2003) was utilized.

THERMICA was used for the generation of the geometric model and computation of radiation exchange factors whereas MSC SINDA was employed for the numerical solution of the discretised energy equation (Eq. 2). Among the numerous solvers embedded in MSC SINDA, a robust and CPU efficient solver based on modified Dufort-Frankel scheme (Moin, 2010) was utilized in the solution. According to this scheme, Eq. (2) is written as

$$\left(1 + \frac{(\Delta t)(G_{ij})}{mc_{p,i}}\right) T_i^{p+1} = T_i^p + \sum_{j=1}^N \frac{(\Delta t)(G_{ij})}{mc_{p,i}} T_j^p - \sum_{j=1}^N \frac{(\Delta t)(G_{ij})}{mc_{p,i}} T_i^{p-1} + \frac{(\Delta t)(q_i)}{mc_{p,i}} \quad (5)$$

where N is the total number of diffusion nodes, i and j are node, $p+1$ is the next (unknown) time level, p is the present time level, $p-1$ is the previous time level, $mc_{p,i}$ is the nodal capacitance of node i , q_i is the source term and G_{ij} is the total conductor which is defined as

$$G_{ij} = C_{i,j} + R_{i,j} (T_i^2 + T_j^2) (T_i + T_j) \quad (6)$$

RESULT AND DISCUSSION

Thermal Vacuum Cycling Test

The modeling effort presented in this study aims to simulate the transient behavior of the ADCU during the TVCT which is performed to verify the performance of the equipment under vacuum and extreme temperatures. The TVCT under consideration was performed at qualification level. This means that device under test was subject to 8 cycles each consisting of hot and cold temperature extremes.

For the measurement of temperatures during TVCT, 10 (ten) Pt100 type temperature sensors were installed at different locations on the ADCU. In order to locate the sensors inside the box, 4 holes having diameter of 1 cm were drilled on the side-walls of the box. The locations of the sensors and their correspondence in the geometrical model are illustrated in Fig. 5 -6. The sensor designated as 7 and mounted on the outer surface of the box was selected as the temperature reference point (TRP) (Fig. 6). TRP is a physical point located on the outer surface of the equipment which represents its thermal status during the TVCT. A TRP is selected on the exterior surfaces of the equipment due to accessibility i.e. there will be no access to the interior of the flight equipment. The second criteria while selecting the location of TRP is its proximity to the component having the possibility of exceeding its operating temperature. For the present investigation this component is the DC-DC converters.

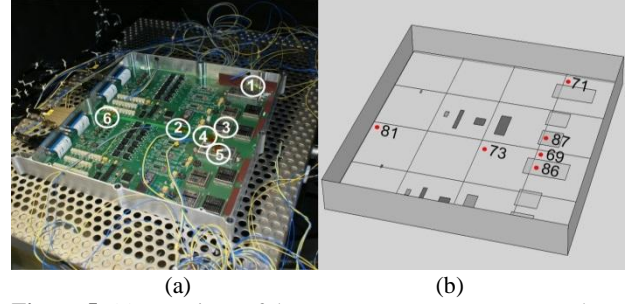


Figure 5. (a) Locations of the temperature sensors mounted on the PCB ; (b) Nodes corresponding to the temperature sensors.

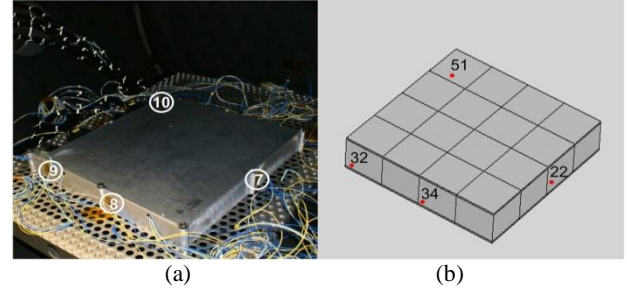


Figure 6. (a) Locations of the temperature sensors mounted on the outer surface of the box ; (b) Nodes corresponding to the temperature sensors.

The objective of the tests is to drive the temperature reference point (TRP) of the equipment to these extremes at each cycle. For the device under test, the hot and cold extremes determined by the European Cooperation for Space Standardization (ECSS) Testing standard (2002) are 323 K and 253 K, respectively.

Description of The Test Problem

Validation of the thermal mathematical model developed in this study was performed by the test measurements obtained in the TVCT described above. Since TVCT is a cyclic process, instead of simulating the whole test, two test cases that are extracted from the sequence were utilized. These test cases are illustrated on the actual test data recorded during the TVCT and shown in Fig. 7. Note that the temperature profile given in the figure is only for the TRP of the ADCU (i.e. sensor 7). Hot case is characterized by the facts that the ADCU is operational (components dissipate heat) and the TRP is driven to the hot temperature extreme (323 K) by adjusting the shroud temperature of the TVC to 293 K. In cold case, the ADCU is non-operational (components do not dissipate heat) and the TRP is driven to the cold temperature extreme (253 K) by adjusting the shroud temperature to 253 K.

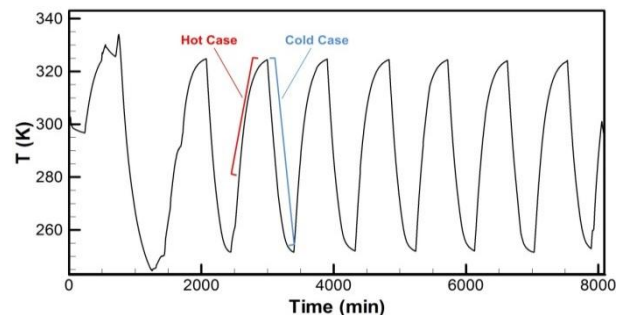


Figure 7. Hot case and cold case

Hot Case

In Fig. 8, transient temperature profiles of various nodes on the ADCU obtained by mathematical model simulations are compared with the test measurements. As expected, the rate of increase in the temperature of nodes 69 and 86 are the highest due to their proximity to the DC-DC converter (see Table 1 and Fig. 5) and they remain to be the hottest nodes at steady state. On the other hand, nodes 34 and 51 have the lowest temperature increase rate since they are located on the exterior surface of the box (facing the cold shroud) and away from the heat dissipation sources. As expected, they are the coldest nodes in the system at steady state.

When the figure is examined, it will be seen that temperatures are overpredicted during the first 10000 s. This is attributed to the fact that the heat dissipations of the PCB components are taken as their maximums (see Table 1) in the mathematical model simulations.

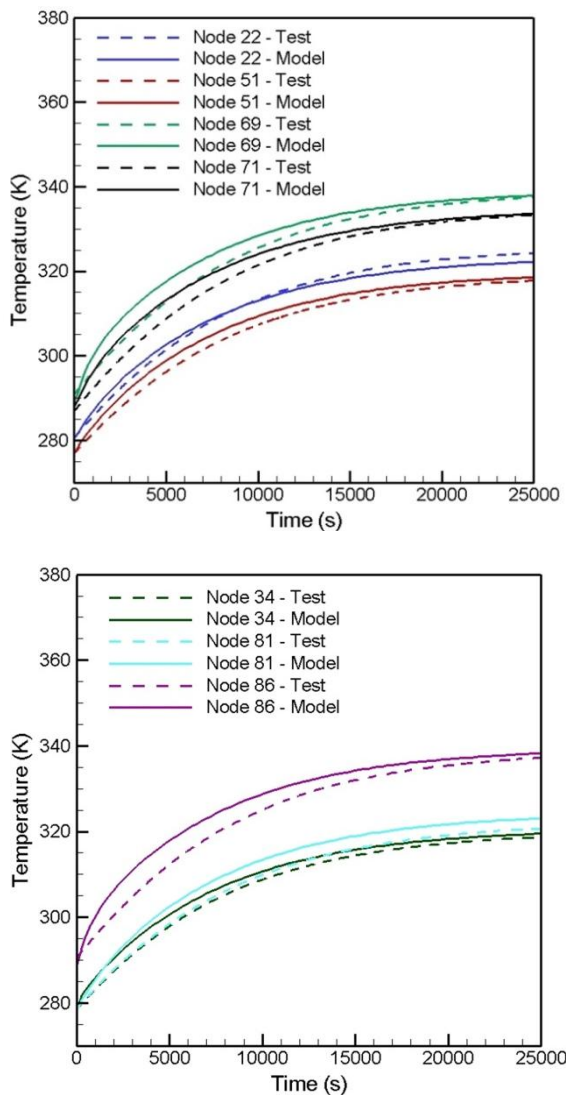


Figure 8. Transient temperature profiles for hot case

However, the actual dissipations during this period are less than their maximums due to their temperature dependence. From this point onward, the discrepancy between the predictions and the measurements tend to decrease owing

to the increase in the actual dissipations with increasing temperature. This effect is best observed for nodes with heat dissipations (69, 71 and 86) and pronounced less for nodes without dissipation (22, 34, 51 and 81).

In order to provide the reader an overall view of the accuracy of the methodology, standard deviation of the transient solution with respect to measurements were calculated using

$$\sigma = \sqrt{\frac{\sum_{i=1}^N (T_{i,c} - T_{i,m})^2}{N-1}} \quad (7)$$

where σ is the standard deviation, N is the total number of nodes for which measurements are available, $T_{i,c}$ and $T_{i,m}$ are the computed and measured temperatures for node i , respectively. The standard deviation as a function of solution time for hot case is illustrated in Fig. 9. In accordance with the temperature profiles displayed in Fig. 8, the discrepancy between the predictions and the measurements are the highest around 3000 s which then starts to decrease as solution progresses as a consequence of the constant heat flux approach explained earlier. Nonetheless, the standard deviation for the whole solution is always less than 5 K as suggested by ECSS.

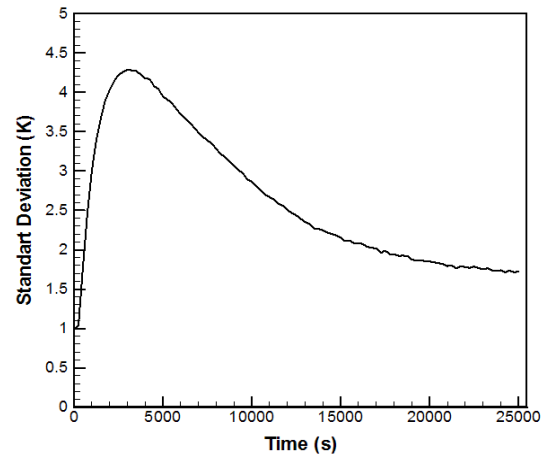


Figure 9. Standard deviation as a function of solution time for hot case

Cold case

As shown in Fig. 7, cold case is the continuation of the hot case in which the ADCU is non-operational. Therefore, the temperatures start from a maximum and then converge to shroud temperature (heat sink) with no significant temperature gradient among the nodes as can be seen in Fig. 10. Furthermore, the discrepancy between the predictions and the measurements observed in the early phases of the hot case simulation is not present in this case due to non-dissipating components. Similar to what has been done for hot case, the standard deviation as a function of solution time for the cold case is calculated and presented in Fig. 11. In contrast to hot case, the standard deviations for cold case exhibit a more random characteristic and vary in a narrower band. Overall

inspection of figure reveals that the deviations remain less than 3 K at all times.

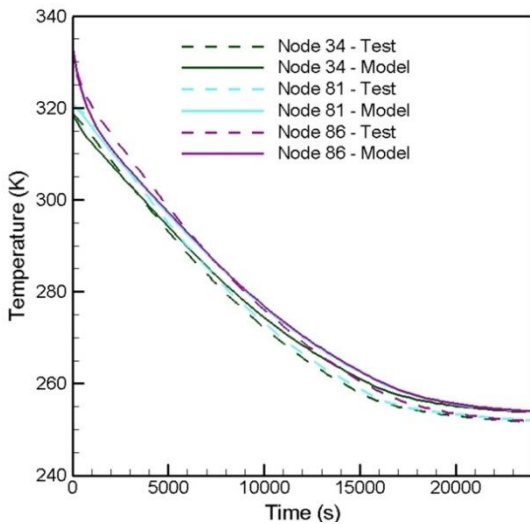
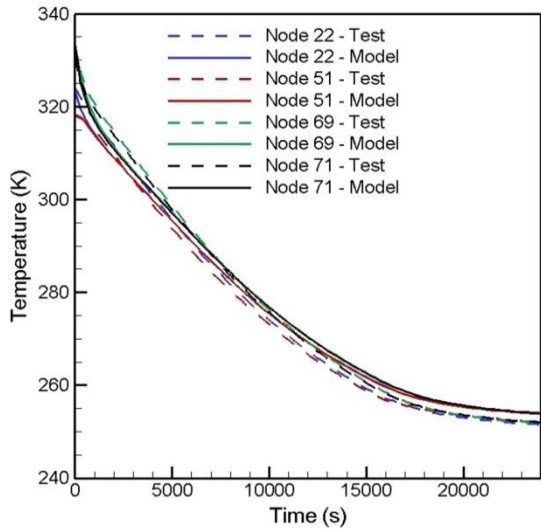


Figure 10. Transient temperature profiles for cold stage

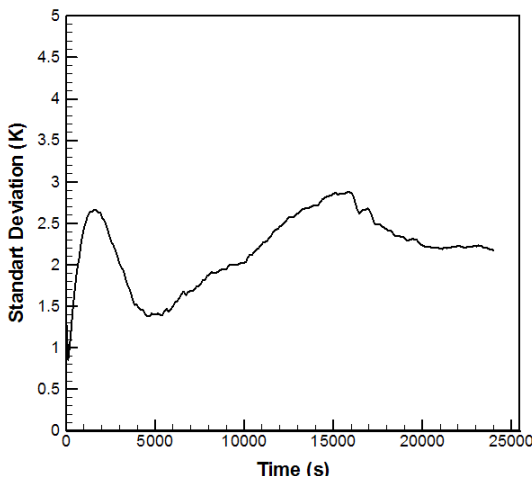


Figure 11. Standard deviation as a function of solution time for the cold case

CONCLUSIONS

In what preceded, development of a thermal mathematical model for the simulation of transient behavior of ADCU in TVC environment was described. The model was based on TNM and simulations were carried out using a commercial thermal analysis software package. The predictive performance of the model was demonstrated on two test cases, hot and cold, that have been extracted from the TVCT of the ADCU by comparing the model predictions with the measurements. The standard deviations calculated between the predictions and the test measurements were found to be less than 5 K for the hot case and less than 3 K for the cold case at all times which indicates that the performance of the developed model was in compliance with the correlation criteria suggested by ECSS. On the whole, the methodology used for the development of the thermal mathematical model within the framework of this study was found to be an accurate and efficient approach which can be used with confidence in the design phases of future spaceborne equipment.

REFERENCES

- Astrium, 2003, SINDA user manual, ver. 3.2.
- Astrium, 2003, THERMICA User Manual, ver. 3.2.
- ECSS-E-10-03A (ESA-ESTEC), 2002, Space Engineering Testing.
- Fujipoly, 2009, SARGON 25G-Tag Data Sheet.
- Gilmore D.G., 2002, Spacecraft Thermal Control Handbook Volume 1: Fundamental Technologies (2nd Ed.), The Aerospace Press, El Segundo, California.
- Kim J.K., Yakayama W., Ito T., Shin S. and Lee S., 2009, Estimation Of Thermal Parameters of The Enclosed Electronic Package System by Using Dynamic Thermal Response, Mechatronics, b19, 1043-1050.
- Oppenheim A.K., 1954, Radiation analysis by the network method, Transaction of ASME, 54.
- Moin P., 2010, Fundamentals of Engineering Numerical Analysis (2nd Ed.), Cambridge University Press, New York.
- Quintero A.H., Welch J.W. and Wolf H., 1999, Perceptiveness of The Thermal Vacuum Testing, In 18th Aerospace Testing Seminar.
- Sartre V. and Lallemand M., 2001, Enhancement of Thermal Contact Conductance For Electronic Systems, Applied Thermal Engineering, 21, 221-235.
- Seo H.S., Rhee J., Han E.S., Kim I.S., 2013, Thermal Failure of The LM Regulator Under Harsh Space Thermal Environments, Aerospace Science and Technology, 27, 49-56.
- Siegel R. and Howell J.R., 2002, Thermal Radiation Heat Transfer, Taylor & Francis, New York.



Cem Ömür

Cem Ömür graduated from Mechanical Engineering Department of Middle East Technical University in 2007. After working at Ford Motor Company between July 2007 and August 2008 as an Engine Test Engineer, he started working in Turkish Aerospace Industry, Inc (TAI). He received his M. Sc. in the year 2010 from the Mechanical Engineering (M.E.) Department of Middle East Technical University. He has expertise in the fields of thermal vacuum testing, instrumentation of sensors and testing diesel engines via dynamometers. He is currently working at TAI as a thermal test engineer and performing his Ph.D. studies at the Mechanical Engineering Department of Gazi University, Ankara, Turkey.



Dr. Ahmet Bilge Uygur

Dr. Ahmet Bilge Uygur graduated from Chemical Engineering Department of Middle East Technical University (Ankara, Turkey) in the year 2000. He received his M. Sc. and Ph. D. degrees from the same department in the years 2002 and 2007, respectively. His principle research interests are Computational Fluid Dynamics, Spacecraft Thermal Control and Design, Thermal Mathematical Model Development and Thermal Vacuum Testing. He is currently the Lead Engineer for Thermal Tests in Turkish Aerospace Industries, Inc.